On the influence of airfoil deviations on the aerodynamic performance of wind turbine rotors

On the influence of airfoil deviations on the aerodynamic performance of wind turbine rotors

J Winstroth and J R Seume

ForWind - Center for Wind Energy Research, Leibniz Universität Hannover,
Institute of Turbomachinery and Fluid Dynamics (TFD), Appelstr. 9, 30167 Hanover, DE

E-mail: winstroth@tfd.uni-hannover.de

Abstract. The manufacture of large wind turbine rotor blades is a difficult task that still involves a certain degree of manual labor. Due to the complexity, airfoil deviations between the design airfoils and the manufactured blade are certain to arise. Presently, the understanding of the impact of manufacturing uncertainties on the aerodynamic performance is still incomplete. The present work analyzes the influence of a series of airfoil deviations likely to occur during manufacturing by means of Computational Fluid Dynamics and the aeroelastic code FAST. The average power production of the NREL 5MW wind turbine is used to evaluate the different airfoil deviations. Analyzed deviations include: Mold tilt towards the leading and trailing edge, thick bond lines, thick bond lines with cantilever correction, backward facing steps and airfoil waviness. The most severe influences are observed for mold tilt towards the leading and thick bond lines. By applying the cantilever correction, the influence of thick bond lines is almost compensated. Airfoil waviness is very dependent on amplitude height and the location along the surface of the airfoil. Increased influence is observed for backward facing steps, once they are high enough to trigger boundary layer transition close to the leading edge.

1. Introduction

Wind turbines convert the kinetic energy contained in the wind into mechanical and hence electrical power. The efficiency of this conversion process is dominated by the aerodynamics of the rotor blades. One common approach to modeling these aerodynamics is to represent the 3D blade with discrete 2D airfoils for a number of radial positions along the span of the rotor. By varying the outer geometry of one or more of these 2D sections, the local aerodynamics of the blade and therefore the efficiency of the entire conversion process is altered. The aerodynamic properties of these 2D airfoils are modeled by polars of lift, drag and moment, usually obtained from wind tunnel experiments or Computational Fluid Dynamics (CFD). No matter how these 2D airfoil polars are generated, the data will most certainly be for ideal airfoil geometries without taking into account the manufacturing process of a wind turbine blade.

Over the last two decades the manufacturing process for modern wind turbine blades has matured significantly. However, manufacturing modern wind turbine blades is not a trivial task due to the enormous size of the blades, the geometric complexity which can involve pre-bend, pre-sweep and blade twist and the heterogeneity of the materials used. The final geometry of the manufactured blade is further affected by the manual labor and fine tuning which is still necessary once the pressure and suction side of the blade are bound together. Therefore, the

geometry of a manufactured wind turbine rotor blade can deviate significantly from its design geometry, which also affects the aerodynamic performance of the wind turbine rotor.

In the past, different authors tried to quantify the impact of airfoil deviations due to manufacturing using different approaches. Loeven and Bijl [1] investigated the impact of airfoil deviations for the NACA 5412 airfoil by means of the probabilistic collocation method. They varied the maximum camber, maximum camber location and the thickness. Their results show a significant influence on both lift and drag. Demuijnck and Kooij [2] investigated the impact of thick bond lines and accumulated dirt at the leading edge on the aerodynamic performance of the DOWEC 6MW wind turbine using RFOIL. They showed that accumulated dirt at the leading edge of an airfoil will alter the lift and drag polars, causing a significant impact on Annual Energy Production (AEP). A similar approach was taken by Ernst et al. [3]. They investigated the influence of airfoil deviations on the lift and drag coefficients of wind turbine airfoils by using a Latin hypercube sampling and XFOIL. In their study, they varied the maximum thickness, the maximum thickness location, the maximum camber, the maximum camber location and the trailing edge thickness of all airfoils of the NREL 5 MW reference wind turbine. Based on their results, the airfoil deviations had significant influence on the damage-equivalent flap-wise bending moments, but only a negligible influence on the AEP. What is common to all studies is that none had access to measured data from manufactured wind turbine blades, and therefore had to rely on assumptions for their inputs.

The present study aims to quantify the influence of airfoil deviations due to manufacturing on the aerodynamic performance of wind turbine rotors. Significant airfoil deviations (ref. Sec. 2) are applied to the four most outer airfoils of the NREL 5MW wind turbine [4]. Polars for both the reference/unmodified airfoils and the modified airfoils are generated by means of 2D Computational Fluid Dynamics (CFD). The power curve of the different rotor blade configurations is estimated based on these polars and the wind turbine analysis code FAST [5] from the National Renewable Energy Laboratory (NREL). Furthermore, the power curves are used to estimate the average power production of the different configurations by assuming an IEC 61400 class $\mathrm{II_B}$ wind distribution [6].

2. Airfoil modifications

The investigated airfoil deviations in this work are based on observations made on manufactured blades and differ significantly from all deviations examined in previous studies. All airfoils are normalized to unity chord length before modification and are renormalized after modification if the chord changes due to the modification. Great care is taken to assure a continuous and smooth surface curvature of the modified airfoils, in order to avoid triggering transition due to surface discontinuity. The following subsections will introduce each modification, present an exemplary sketch showing the original and the modified airfoil and explain the reasoning behind each modification.

2.1. Mold tilt towards the leading edge

The modification is shown in Figure 1a. The airfoil is split into suction side and pressure side at the leading edge. Afterwards, the suction side is rotated counterclockwise and the pressure side is rotated clockwise about the leading edge point. The amount of rotation for each side is always the same. To fix the curvature discontinuity at the leading edge, a few points on the suction and pressure side close to the leading edge are removed and later reintroduced by fitting a smoothing B-spline through the remaining points defining the airfoil.

The deviation might occur if the spar of the blade or the bonds connecting the spar to the outer shell of the blade are too thick when joining the suction and pressure side. It is identified by the abbreviation *RotLEX* throughout this paper, where X denotes the total amount of rotation about the leading edge point (pressure-side rotation + suction-side rotation = X).

2.2. Mold tilt towards the trailing edge
The modification is shown in Figure 1b. The procedure is the same as for the mold tilt towards the leading edge except, the rotation is about the trailing edge point of the airfoil. To avoid a flat leading edge, a few points on the suction and pressure side close to the leading edge are removed, a new point at (0, 0) is added and a smoothing B-spline is fitted to these points.

The deviation might occur if the spar of the blade or the bonds connecting the spar to the outer shell of the blade are too thick when joining the suction and pressure side. It is identified by the abbreviation *RotTEX* throughout this paper, where X denotes the total amount of rotation about the trailing edge point (pressure-side rotation + suction-side rotation = X).

2.3. Step change
The modification is shown in Figure 1c. A backward facing step is applied on the suction and pressure side of the airfoil at $0.05c$. On a wind turbine blade, backward facing steps can occur due to the application of protective tapes at the leading edge of the blade. Throughout this work, the step change modification is identified by the abbreviation *StepXx0.05*, where X denotes the height of the backward facing step normal to the surface of the airfoil in terms of unit chord.

2.4. Sine wave
The modification is shown in Figures 1d - 1h for different locations along the surface of the airfoil. The two period sine wave has an extend of $0.2c$, where c is the chord length of the airfoil. It represents the waviness often seen on manufactured blades at different locations on the surface. Throughout this work the sine wave modification is identified by the abbreviation *SWuB-EaXp2.0*, where X is the amplitude of the sine wave in terms of unit chord. B and E denote the start and end point of the modification along the surface of the airfoil in terms of coordinate u, which runs from the rear-most suction-side point to the rear most pressure side point and is normalized to unity.

2.5. Thick bond lines
The modification is shown in Figure 1i. It takes into account thick bond lines by translating the suction side into the positive y-direction and the pressure side into the negative y-direction. The amount of translation for each side is always equal. To avoid a flat leading edge, a few points on the suction and pressure side close to the leading edge are removed, a new point at (0, 0) is added and a smoothing B-spline is fitted to these points. Throughout this work the thick bond lines modification is identified by the abbreviation *TBLX*, where X is the total amount of translation in terms of chord length (suction-side translation + pressure-side translation = X).

2.6. Thick bond lines with cantilever correction
The modification is shown in Figure 1j. It is similar to the thick bond lines modification but does involve an extra correction step. First, the suction side and the pressure side are translated apart by an equal amount. Then a section from $0.25c$ to $0.5c$ on the suction and on the pressure side is chosen to remain fixed. However, the forward and rearward facing points from the fixed section are bent downwards on the suction side and upwards on the pressure side until the trailing edge and leading edge points are back to their original position. The bending line used for this transformation is that of a cantilever beam with origin at the ends of the fixed sections.

Throughout this work the thick bond lines with cantilever correction modification is identified by the abbreviation *TBLCX*, where X is the total amount of translation in terms of chord length (suction-side translation + pressure-side translation = X). This airfoil modification follows the same reasoning as the thick bond lines modification, but assumes that the forward and rearward facing parts of the airfoil are forced back into their original position by bending the suction and pressure side of the airfoil.

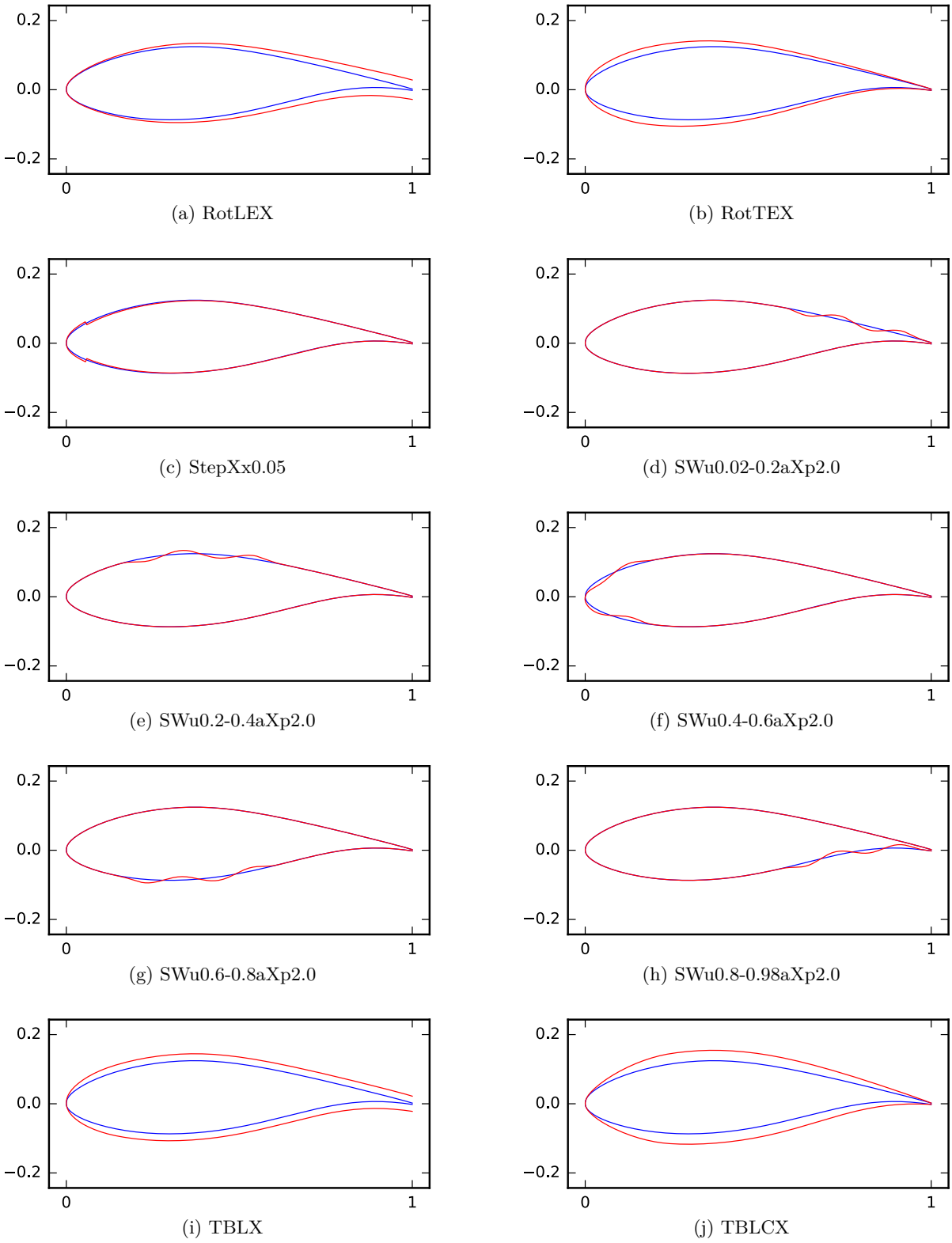

(a) RotLEX (b) RotTEX

(c) StepXx0.05 (d) SWu0.02-0.2aXp2.0

(e) SWu0.2-0.4aXp2.0 (f) SWu0.4-0.6aXp2.0

(g) SWu0.6-0.8aXp2.0 (h) SWu0.8-0.98aXp2.0

(i) TBLX (j) TBLCX

Figure 1: Examples of original (blue) and modified airfoils (red) investigated in this work.

3. Approach and methods

This section outlines the approach taken to investigate the influence of different airfoil modifications on the aerodynamic performance of the NREL 5MW wind turbine in onshore configuration. The influence of different airfoil deviations on the aerodynamics is modeled based on lift, drag and moment polars generated from CFD simulations using the solver Ansys Fluent. These polars are then used as input to AeroDyn, in order to estimate the power curves of the NREL 5MW wind turbine for different rotor configurations using the software FAST from NREL. Finally, the power curves are used to evaluate the average power, AEP and annual loss in kWh and Euros based on a IEC 61400 class $\mathrm{II_B}$ wind distribution. More details about each step in the analysis is provided in the following subsections.

3.1. Modified airfoils and applied modifications

The four most outer airfoils of the NREL 5MW blade (DU 97-w-300, DU 91-w2-250, DU 93-w-210 and NACA 64-618) are modified in this work. They represent approximately 60% of the outer part of the blade. Table 1 summarizes the modifications investigated for each of the four airfoils. Please refer to Section 2 for a detailed description of each modification and the used abbreviations.

Table 1: Modifications applied to each of the four outer airfoils of the NREL 5MW blade.

Modification name	List of X-values	Unit
RotLEX	1.0, 1.5, 2.0, 3.0	deg
RotTEX	1.0, 1.5, 2.0, 3.0	deg
Step$X$x0.05	0.0001, 0.0003, 0.0006, 0.001	chord
SWu0.02-0.2aXp2.0	0.001, 0.003, 0.005, 0.01	chord
SWu0.2-0.4aXp2.0	0.001, 0.003, 0.005, 0.01	chord
SWu0.6-0.8aXp2.0	0.001, 0.003, 0.005, 0.01	chord
SWu0.8-0.98aXp2.0	0.001, 0.003, 0.005, 0.01	chord
TBLX	0.003, 0.005, 0.01, 0.02	chord
TBLCX	0.005, 0.01, 0.02, 0.03	chord

3.2. CFD simulations and airfoil polars

The polars of lift, drag and moment for each modification are generated by means of 2D CFD simulations. Each modification is simulated using the k-ω-SST model to get a fully turbulent polar, and also using the k-ω-SST model combined with the γ-Re_θ transition model to get a polar that takes into account the transition process of the boundary layer. Both results are then blended into a single polar using a weighting factor of 0.7 for the simulation with transition and 0.3 for the fully turbulent simulation. The weighting factors are a rough guess of the authors based on the weather conditions in northern Germany. The resulting polar is used as input for AeroDyn.

This approach is used to consider the fact that wind turbines operate in an uncontrolled environment. Therefore, the rotor can operate either in a clean state with maximum efficiency, or in a state with dirt build-up at the leading edge which can trigger the transition process and degrade the rotor efficiency. A good design must consider both rotor conditions in order to be efficient over the full life-cycle of the wind turbine.

3.2.1. Numerical grid A structured grid with a C-topology is used with 385 nodes along the surface of the airfoil and 141 nodes in the wake of the airfoil. The far field boundaries are $50c$ away from the airfoil. To ensure good boundary layer resolution, the wall distance of the first node is set to satisfy $y^+ \leq 0.75$. The expansion ratio away from the airfoil surface is 1.1 and the total cell count is $\approx$ 100k. Figure 2 shows a close up view of the numerical grid close to the airfoil surface.

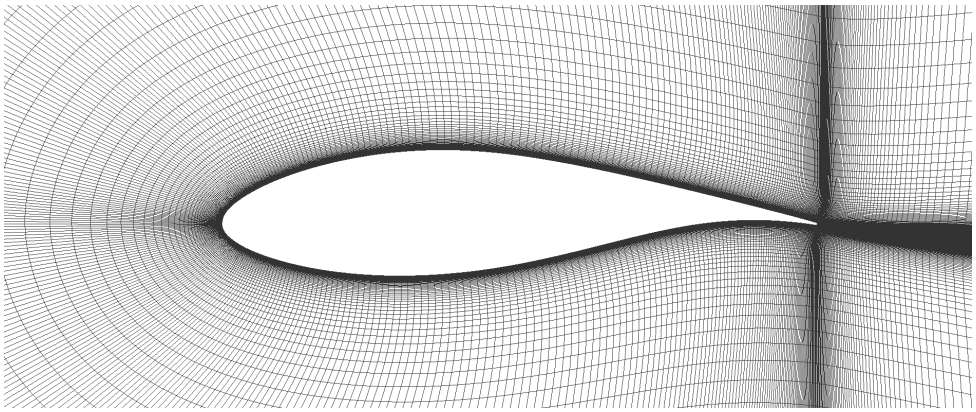

Figure 2: Close up view of the numerical grid.

3.2.2. Boundary conditions The boundary conditions of the 2D CFD simulations are derived from the NREL 5MW turbine operating at rated power for $T = 288.15$ K. This corresponds to a wind velocity of 11.4 m/s, and a rotational speed of the rotor of 12.1 rpm. Both the simulation of the reference airfoil (airfoil without modification) and the simulations of all its modifications always apply the same boundary conditions as listed in Table 2. Since all simulations are run with unity chord length, the pressure is used to obtain Reynolds number similarity. Please note that airfoils and their modifications will be identified by their abbreviation from this point on (cf. Table 2).

Table 2: Boundary conditions for simulated airfoils and their modifications.

Name	Abbreviation	Pressure [Pa]	Reynolds number [-]	Mach number [-]
DU 99-w-405	du40	459475.9	5.82E+06	0.0551
DU 99-w-350	du35	458381.9	7.87E+06	0.0746
DU 97-w-300	du30	428420.7	9.41E+06	0.0956
DU 91-w2-250	du25	390149.1	1.05E+07	0.1173
DU 93-w-210	du21	340072.3	1.15E+07	0.1468
NACA 64-618	naca64	231907.4	1.08E+07	0.2029

3.3. FAST simulations
FAST v8.12.00a-bjj in combination with AeroDyn v15.00.00b-bjj is used to calculate the power curves for different airfoil deviations. The general setup of the NREL 5MW configuration is based

on the certification test 26 that is supplied with the FAST source code. Three minor changes are made to the configuration files supplied with test 26. First, ElastoDyn is used instead of BeamDyn to reduce CPU time. Second, the FAST time step is changed to $DT = 0.01\,\mathrm{s}$. Third, the blade configuration for AeroDyn is changed. Instead of using 19 blade nodes to discretize the blade, 62 blade nodes are used. These 62 nodes are distributed uniformly in intervals of 1 m along the radial span of the blade. By increasing the number of nodes, the influence of different airfoil deviations and the influence of their spanwise extend can be tested in greater detail.

To calculate the power curve for each modification, a 2 min FAST simulation is run for each wind speed, starting from the cut-in wind speed of 3 m/s and incrementing the wind speed in steps of 1 m/s for each consecutive simulation until rated power is reached. For wind speeds higher than the wind speed where rated power is reached, rated power is assumed until the cut-out wind speed of 25 m/s is reached. After each simulation the wind turbine power for the corresponding wind speed is calculated by averaging the generator power output from FAST over the last minute of the simulation. The wind speed is set at hub height. A steady wind condition including wind shear is used but turbulence is not considered. The wind shear is modeled by the power law with an exponent of 0.143.

In order to compare all modifications to a common reference, a reference power curve is established based on polars generated from 2D CFD simulations of the unmodified airfoils listed in Table 2. The power curves for each modification are generated according to the following procedure:

(1) Replace the reference polar at $r = 30\,\mathrm{m}$ with the polar of the modification and calculate the power curve.
(2) Replace the reference polar at $r = 29\,\mathrm{m}$ and $r = 30\,\mathrm{m}$ with the polar of the modification and calculate the power curve.
(3) Replace the reference polar at $r = 29\,\mathrm{m}$, $r = 30\,\mathrm{m}$ and $r = 31\,\mathrm{m}$ with the polar of the modification and calculate the power curve.
(4) Increase the spanwise extend of the modification in this manner until the total extend of the modification is 20 m.
(5) Repeat steps (1) - (4) starting at spanwise positions $r = 40\,\mathrm{m}$ and $r = 50\,\mathrm{m}$

A total of 60 different power curves are calculated based on this procedure for each modification. Therefore, permitting to rate the severity of the airfoil deviation at different spanwise positions with varying spanwise extent.

3.4. Average power and Annual Energy Production

The power curves are used to estimate the average power and the AEP of the NREL 5MW wind turbine for a IEC 61400 class $\mathrm{II_B}$ wind distribution. The wind distribution is represented using a Weibull distribution with a scale factor of $c = 9.59$ and an exponent of $k = 2$, which corresponds to a mean wind speed of $\overline{U} = 8.5\,\mathrm{m/s}$. The average wind turbine power

$$\overline{P}_W = \sum_{i=1}^{N_B} \left\{ \exp\left[-\left(\frac{U_{i-1}}{c} \right)^k \right] - \exp\left[-\left(\frac{U_i}{c} \right)^k \right] \right\} P_W \left(\frac{U_{i-1} + U_i}{2} \right),$$

is estimated, where N_B are the wind bins starting at 3 m/s up to 25 m/s and P_W is the power curve of the wind turbine evaluated at the middle of the wind bin interval.

Once the average power $\overline{P}_W$ for the wind distribution is known, the Annual Energy Production

$$AEP = \overline{P}_W \cdot 8760$$

is calculated. By comparing the AEP of the reference to the AEP of the modifications, the annual loss in kWh for each modification is estimated and also expressed in terms of incurred losses in Euros.

4. Results and discussion

The results of this work are tabulated. A general explanation on how to read and interpret these tables is given in the first part of this section. The second part focuses on discussing the impact of different airfoil deviations at the outermost 30 % of the blade.

4.1. General format for presentation of results

Tables A1 and A2 in the appendix provide examples of the general format used to present the overall results. However, due to the number of different airfoil deviations and turbine setups investigated and the limited space available, only a fraction of the overall results can be shown here. Nevertheless, the authors took great care to include the most valuable results into this paper and the complete data set is available online in the form of Excel sheets on the companion homepage to this paper. In addition, the point coordinates for all airfoil modifications and their polars are also available for download.

The general structure of the result tables is explained based on Tables A1 and A2. The first column identifies the modification by its abbreviation (cf. Section 2), where *Reference* is the unmodified airfoil. In the next three columns (2-4), the location of the maximum lift-to-drag ratio $\alpha_{(L/D)_{max}}$, the maximum lift-to-drag ratio $(L/D)_{max}$ and a mean lift-to-drag ratio $(L/D)_{mean}$ are listed. The mean lift-to-drag ratio is determined by:

(1) Finding the maximum lift-to-drag ratio $(L/D)_{max}$ of the unmodified reference airfoil.
(2) Defining an angle of attack (AOA) interval for the unmodified reference airfoil so that the lower AOA α_{lower} corresponds to $(L/D)_{lower} = (L/D)_{max} - 2.5$ and the upper AOA α_{upper} corresponds to $(L/D)_{upper} = (L/D)_{max} - 2.5$ with $\alpha_{lower} < \alpha_{upper}$.
(3) Calculating $(L/D)_{mean}$ for the reference and all modifications by taking the mean of (L/D) in the interval $\alpha_{lower} \leq \alpha \leq \alpha_{upper}$.

It is important to note that the interval $\alpha_{lower} \leq \alpha \leq \alpha_{upper}$ for a given reference airfoil and all its modifications is constant and based only on the lift-to-drag curve of the reference airfoil. The reasoning behind $(L/D)_{mean}$ is that the wind turbine blade is designed to operate at an AOA close to the maximum lift-to-drag ratio of the reference airfoil. Therefore, the interval $\alpha_{lower} \leq \alpha \leq \alpha_{upper}$ defined by the reference airfoil is of particular interest. The name of the reference airfoil, on which all modifications are based, is given in the first row above columns (2-4).

In the next columns, information for different wind turbine blade configurations are presented. Tables A1 and A2 for example shows the average power loss relative to the reference in percent for different modifications and their different spanwise extents on the wind turbine blade. The numbers in the second row above each column define the spanwise extent of the modification in meters. Here is an example to make this clearer (cf. Table A1): In the fifth row, the name of the modification is *RotLE1.0* and the base or reference airfoil to which this modification is applied is *NACA 64-618*. The lift-to-drag curve for this modification has a maximum at $\alpha_{(L/D)_{max}} = 5.07$ of $(L/D)_{max} = 95.03$ and a $(L/D)_{mean} = 93.90$. If this modification is applied from $r = 46.0\,\mathrm{m}$ to $r = 56.0\,\mathrm{m}$ (denoted by 46-56 in the table) along the wind turbine blade, the average power loss relative to the reference is $-0.486\,\%$. If this modification is applied from $r = 42.0\,\mathrm{m}$ to $r = 61.5\,\mathrm{m}$ (denoted by 42-61.5 in the table) along the wind turbine blade, the average power loss relative to the reference is $-0.821\,\%$.

Tables A1 and A2 only have information for one airfoil (*NACA 64-618*) because the modified blade areas consist of only this one airfoil. If the modified blade areas of the blade are made of more than one airfoil, the table or Excel sheet includes each of these airfoils.

4.2. Airfoil deviations at the outer 30 % *of the blade*

The influence of airfoil deviations at the outer 30 % of the NREL 5MW blade are presented in Tables A1 and A2. The most severe modification with a relative power loss of $-2.392\,\%$ is *RotLE3.0*. For this modification, the considerable increase in trailing edge thickness leads to a high increase in drag. When comparing the *RotLEX* modifications to one another, a continuous increase in relative power loss with increasing rotation angle is observed. When comparing the *RotLEX* modifications to all other modifications, it becomes obvious that even the smallest rotation angle of 1 deg, results in an average power loss that is higher than the loss for most other modifications. The relative loss in power generation of the *RotTEX* modifications, which lead to an increase in thickness towards the leading edge, is generally a lot smaller than for the *RotLEX* modifications. However, the losses also increase with increasing rotation angle.

The results of the *StepXx0.05* modifications also show an increase in relative power loss with increasing step heights. However, there is a drastic increase when going from a step height of $0.0001c$ to $0.0003c$. A step height of $0.0001c$ with a relative power loss of $-0.013\,\%$ has almost no influence while the next step height results into a noticeable power loss of $-0.548\,\%$. This is due to the fact that the lowest step height, unlike all other step heights, does not trigger boundary layer transition. Once boundary layer transition is triggered by the step, a further increase in step height does not result in significantly more power loss. Compared to all other modifications, a step change modification that does trigger boundary layer transition, ranks among the middle when comparing relative power loss.

Looking at all sine wave modifications, the general trend is an increase in power loss with an increase in sine wave amplitude. With the exception of *SWu0.2-0.4a0.005p2.0* and *SWu0.4-0.6a0.005p2.0*, all sine wave modifications with amplitudes of $0.001c$, $0.003c$ and $0.005c$ have only marginal influence on the power loss. However, at the highest amplitude of $0.01c$, the influence becomes severe, especially for *SWu0.02-0.2a0.01p2.0* and *SWu0.2-0.4a0.01p2.0* which rank among the top 4 modifications with the highest loss in power.

Among the sine wave modifications, two sine wave positions (*du21SWu0.02-0.2aXp2.0* and *du21SWu0.4-0.6aXp2.0*) are especially interesting. Modifications *du21SWu0.02-0.2aXp2.0* show the most severe increase in power loss when going from sine wave amplitude $0.001c$ to $0.01c$. The three lower amplitudes have only a negligible influence, whereas the highest amplitude has the third highest influence on power loss of all modifications. Therefore, the high amplitudes on the suction side toward the trailing edge of the airfoil, have an influence comparable to increased trailing edge thicknesses, which cause extra drag. Modifications *du21SWu0.4-0.6aXp2.0* are interesting because the influence on power loss is rather small, even though the modified area along the surface of the airfoil covers the entire leading edge, which is normally very sensitive to deviations. The results show that backward facing steps that trigger transition at the leading edge are worse than airfoil waviness in this area. However, once the amplitude of the sine wave is $> 0.005c$, the influence on power loss becomes almost equal to a step change modification.

All bond line modifications have a significant influence on the relative power loss. The negative influence on the power loss increases with increasing translation length. Among all modifications, *TBLX* has the second greatest influence on power loss, only surpassed by *RotLEX*. Interestingly, the negative influence can almost be compensated by applying the cantilever correction. For smaller translation lengths of $0.005c$ and $0.01c$, the cantilever correction even results in an increase in average power production. However, at translation lengths $< 0.01c$ the average power production goes below the reference again.

5. Conclusions

This work analyzes a total of 40 different airfoil deviations for 4 different airfoils of the NREL 5MW blade. Polars for the unmodified reference airfoils and all their modifications are generated by means of CFD, and used as input to FAST in order to generate power curves for over 2400 different blade configurations. Based on these power curves, the average power production of the different blade configurations is estimated and used to investigate the influence of each modification.

The most severe influence on average power production have the mold tilt towards the leading edge modifications (*RotLEX*), closely followed by the thick bond lines modifications (*TBLX*). However, the negative influence of the *TBLX* modifications can almost be compensated by applying the cantilever correction (*TBLC*). Applying this correction can even have a positive influence on the average power production.

The modifications, mold tilt towards the trailing edge (*RotTEX*), have only a small influence on the average power production, especially when compared to the influence of the *RotLEX* modifications. The backward facing step modifications at the leading edge start having a noticeable influence on the average power productions once the step is high enough to trigger boundary layer transition, which starts at step heights of $\geq 0.0003c$.

For the sine wave modifications, the influence is generally small for the lower amplitudes of $0.001c$, $0.003c$ and $0.005c$. However, at the highest amplitude of $0.01c$, it becomes quite significant. Especially if the sine wave is located on the suction side close to the point of maximum thickness or towards the trailing edge. The area around the leading edge of the airfoil appears less sensitive to airfoil waviness than the suction side for higher amplitudes. However, for small amplitudes, the influence at the leading edge is more severe than on the suction side.

The overall influence of airfoil deviations on the average power production seams rather small. Nevertheless, the most severe modification in this work (*RotLE3.0*) causes an average power loss of $-2.392\,\%$. Assuming a revenue of 8.9 Cent/kWh this translates into an annual loss in revenue of k€ 41.9 p.a. for the NREL 5MW wind turbine and a IEC 61400 class $\mathrm{II_B}$ wind distribution.

Further studies will include data of measured wind turbine airfoils and will look at other airfoil fitness indicators besides the lift-to-drag ratio. The influence of airfoil deviations on the damage equivalent loads is also of particular interest to the authors and will be dealt with in the future.

Acknowledgments

The authors gratefully acknowledge the financial funding by the Federal Ministry for Economic Affairs and Energy (BMWi), Germany under Grand Number 0325792. The work presented was motivated in part by Collaboration Research Center (CRC) 871 "Regeneration of Complex Capital Goods" funded by DFG, the German Research Foundation. We thank our colleagues here at TFD for the valuable discussions concerning the results of this work.

Appendix

Table A1: Influence of different airfoil deviations with varying radial extends at the outer 30 % of the blade - Part I/II

	NACA 64-618 (naca64) airfoil			Average power loss						
	$\alpha_{(L/D)_{max}}$	$(L/D)_{max}$	$(L/D)_{mean}$	51-51	49-53	48-55	46-56	45-58	43-59	42-61.5
Modification name	[deg]	[-]	[-]	[%]	[%]	[%]	[%]	[%]	[%]	[%]
Reference	4.43	111.67	110.65	0	0	0	0	0	0	0
RotLE1.0	7.46	96.14	93.90	-0.048	-0.239	-0.370	-0.486	-0.632	-0.757	-0.821
RotLE1.5	7.12	91.78	90.36	-0.065	-0.320	-0.494	-0.648	-0.841	-1.005	-1.087
RotLE2.0	7.27	86.10	82.81	-0.089	-0.437	-0.675	-0.888	-1.152	-1.377	-1.492
RotLE3.0	8.71	75.95	69.63	-0.143	-0.697	-1.077	-1.410	-1.833	-2.199	-2.392
RotTE1.0	5.44	105.14	104.48	-0.007	-0.035	-0.055	-0.074	-0.100	-0.126	-0.141
RotTE1.5	6.10	105.17	103.19	-0.010	-0.052	-0.082	-0.110	-0.150	-0.187	-0.209
RotTE2.0	6.21	105.59	102.80	-0.011	-0.057	-0.089	-0.120	-0.163	-0.204	-0.229
RotTE3.0	5.97	104.22	100.64	-0.014	-0.071	-0.112	-0.151	-0.206	-0.259	-0.292
Step0.0001x0.05	4.04	109.05	108.32	0.000	-0.002	-0.004	-0.005	-0.007	-0.011	-0.013
Step0.0003x0.05	8.27	99.22	90.96	-0.027	-0.134	-0.209	-0.283	-0.386	-0.486	-0.548
Step0.0006x0.05	8.66	96.72	89.72	-0.028	-0.142	-0.222	-0.299	-0.409	-0.514	-0.580
Step0.001x0.05	7.49	94.45	88.27	-0.030	-0.151	-0.235	-0.318	-0.434	-0.546	-0.616
SWu0.02-0.2a0.001p2.0	4.77	111.06	110.23	0.000	-0.002	-0.003	-0.004	-0.006	-0.008	-0.010
SWu0.02-0.2a0.003p2.0	4.39	109.69	108.87	-0.002	-0.012	-0.019	-0.025	-0.033	-0.040	-0.044
SWu0.02-0.2a0.005p2.0	4.58	104.64	103.81	-0.008	-0.040	-0.062	-0.083	-0.113	-0.140	-0.157
SWu0.02-0.2a0.01p2.0	5.04	71.97	70.85	-0.060	-0.299	-0.463	-0.625	-0.845	-1.062	-1.197
SWu0.2-0.4a0.001p2.0	4.94	110.73	109.21	-0.002	-0.013	-0.021	-0.029	-0.041	-0.052	-0.059
SWu0.2-0.4a0.003p2.0	5.09	109.25	106.19	-0.008	-0.040	-0.063	-0.086	-0.119	-0.150	-0.169
SWu0.2-0.4a0.005p2.0	4.34	99.34	98.50	-0.014	-0.071	-0.111	-0.149	-0.203	-0.255	-0.286
SWu0.2-0.4a0.01p2.0	5.31	74.59	73.26	-0.060	-0.299	-0.464	-0.623	-0.843	-1.054	-1.182

Table A2: Influence of different airfoil deviations with varying radial extends at the outer 30 % of the blade - Part II/II

	NACA 64-618 (naca64) airfoil			Average power loss						
	$\alpha_{(L/D)_{max}}$	$(L/D)_{max}$	$(L/D)_{mean}$	51-51	49-53	48-55	46-56	45-58	43-59	42-61.5
Modification name	[deg]	[-]	[-]	[%]	[%]	[%]	[%]	[%]	[%]	[%]
Reference	4.43	111.67	110.65	0	0	0	0	0	0	0
SWu0.4-0.6a0.001p2.0	5.82	111.43	109.37	-0.002	-0.013	-0.021	-0.028	-0.039	-0.049	-0.055
SWu0.4-0.6a0.003p2.0	5.55	108.84	105.46	-0.008	-0.044	-0.068	-0.093	-0.128	-0.162	-0.182
SWu0.4-0.6a0.005p2.0	5.01	99.22	97.77	-0.015	-0.078	-0.121	-0.164	-0.226	-0.285	-0.322
SWu0.4-0.6a0.01p2.0	6.86	90.13	85.61	-0.032	-0.159	-0.247	-0.334	-0.457	-0.578	-0.654
SWu0.6-0.8a0.001p2.0	4.68	110.83	110.15	0.000	0.000	-0.001	-0.001	-0.002	-0.003	-0.004
SWu0.6-0.8a0.003p2.0	4.83	107.05	106.03	-0.005	-0.026	-0.041	-0.056	-0.076	-0.096	-0.108
SWu0.6-0.8a0.005p2.0	4.62	106.17	105.30	-0.005	-0.029	-0.045	-0.061	-0.084	-0.105	-0.119
SWu0.6-0.8a0.01p2.0	5.01	99.12	97.79	-0.019	-0.097	-0.150	-0.202	-0.273	-0.338	-0.376
SWu0.8-0.98a0.001p2.0	4.74	111.07	110.35	0.000	-0.002	-0.003	-0.004	-0.005	-0.007	-0.007
SWu0.8-0.98a0.003p2.0	4.70	111.28	110.38	-0.004	-0.022	-0.034	-0.045	-0.056	-0.065	-0.068
SWu0.8-0.98a0.005p2.0	4.71	110.51	109.58	-0.007	-0.036	-0.056	-0.072	-0.092	-0.107	-0.114
SWu0.8-0.98a0.01p2.0	6.91	95.44	94.01	-0.019	-0.094	-0.147	-0.200	-0.274	-0.348	-0.394
TBL0.003	6.20	103.86	99.96	-0.026	-0.130	-0.203	-0.269	-0.355	-0.430	-0.471
TBL0.005	5.34	97.41	96.29	-0.035	-0.175	-0.272	-0.358	-0.469	-0.565	-0.614
TBL0.01	6.40	91.79	88.88	-0.061	-0.302	-0.467	-0.614	-0.802	-0.964	-1.048
TBL0.02	7.57	85.64	79.38	-0.109	-0.536	-0.827	-1.086	-1.405	-1.680	-1.821
TBLC0.005	4.89	111.01	109.53	0.002	0.010	0.015	0.018	0.019	0.018	0.015
TBLC0.01	5.42	110.69	108.70	0.003	0.014	0.022	0.026	0.028	0.026	0.020
TBLC0.02	6.04	104.78	100.51	0.002	0.005	0.009	0.005	-0.005	-0.028	-0.051
TBLC0.03	6.62	96.56	89.96	-0.005	-0.030	-0.042	-0.067	-0.101	-0.162	-0.213

References

[1] Loeven G and Bijl H 2008 *Airfoil Analysis with Uncertain Geometry using the Probabilistic Collocation method 49th AIAA/ASME/ASCE/AHS/ASC Structures, Structural Dynamics, and Materials Conference* (Schaumburg, IL, USA)
[2] Demuijnck W and Kooij J 2003 *The effect of profile deviations of the DOWEC 6MW blade on wind turbine power production Task 14 report DOWEC 10078rev1* (Energy Research Center of the Netherlands)
[3] Ernst B, Schmitt H and Seume J R 2014 *Effect of Geometric Uncertainties on the Aerodynamic Characteristic of Offshore Wind Turbine Blades Journal of Physics: Conference Series* **555** 012033
[4] Jonkman J, Butterfield S, Musial W and Scott G 2009 *Definition of a 5-MW reference wind turbine for offshore system development NREL/TP-500-38060* (National Renewable Energy Laboratory)
[5] Jonkman J 2015 *FAST v8* https://nwtc.nrel.gov/FAST
[6] IEC 61400-1 third edition 2005 *Wind turbines - Part1: Design requirements* (International Electrotechnical Commission)